Binding Energies of O_2 and CO to Small Gold, Silver, and Binary Silver−Gold Cluster Anions from Temperature Dependent Reaction Kinetics Measurements

Thorsten M. Bernhardt,*,† Jan Hagen,‡,§ Sandra M. Lang,† Denisia M. Popolan,† Liana D. Socaciu-Siebert,‡,⊥ and Ludger Wöste‡

Institut für Oberflächenchemie und Katalyse, Universität Ulm, 89069 Ulm, Germany, and Institut für Experimentalphysik, Freie Universität Berlin, Arnimallee 14, 14195 Berlin, Germany

Received: November 15, 2008; Revised Manuscript Received: January 8, 2009

A detailed analysis of experimentally obtained temperature-dependent gas-phase kinetic data for the oxygen and carbon monoxide adsorption on small anionic gold (Au_n^-, $n = 1-3$), silver (Ag_n^-, $n = 1-5$), and binary silver−gold ($Ag_nAu_m^-$, $n + m = 2, 3$) clusters is presented. The Lindemann energy transfer model in conjunction with statistical unimolecular reaction rate theory is employed to determine the bond dissociation energies E_0 of the observed metal cluster complexes with O_2 and CO. The accuracy limits of the obtained binding energies are evaluated by applying different transition-state models. The assumptions involved in the data evaluation procedure as well as possible sources of error are discussed. The thus-derived binding energies of O_2 to pure silver and binary silver−gold cluster anions are generally in excellent agreement with previously reported theoretical values. In marked contrast, the binding energies of O_2 and CO to Au_2^- and Au_3^- determined via temperature-dependent reaction kinetics are consistently lower than the theoretically predicted values.

1. Introduction

The chemical reactions of nanoparticles and mass-selected clusters of gold have attracted considerable research interest in recent years,[1−5] motivated by the discovery of the surprising catalytic activity of oxide-supported gold particles.[6−8] Also, the investigations of free mass-selected gold clusters, both experimentally as well as theoretically, have provided a great deal of insight into the unexpected size-dependent chemical and catalytic properties of nanoscale gold (see, e.g., ref 9). In particular, the comparison of clusters of the noble metals gold and silver revealed the unique features of gold and the important role of relativistic effects in the chemistry of this element.[10−18]

For the case of free negatively charged gold clusters, the catalytic oxidation of CO to CO_2 by molecular oxygen has been reported to proceed on Au_2^- [19] as well as on Au_6^-.[20] Anionic gold oxide clusters were also found to oxidize CO.[21−24] For silver cluster anions, indications of catalytic activity in this reaction have been observed for Ag_7^-, Ag_9^-, and Ag_{11}^-.[25] Still, experimental binding energies of catalytically important molecules, such as CO and O_2, to clusters of gold and silver as well as mixtures thereof are rather sparse,[26−32] which is in marked contrast to a vast literature on theoretical predictions of such values.[28,33−56]

Therefore, in this contribution, we present a detailed evaluation of temperature-dependent gas-phase reaction rate constants of the reactions of O_2 and CO with small mass-selected noble metal cluster anions that have been determined in our laboratory[16,19,25,29,57−61] with the aim to derive reliable experimental values for the binding energies of these molecules to the clusters. For this purpose, a strong emphasis is put on the discussion of the data evaluation procedure and the possible sources of error in the determined binding energies. As a striking result, we are able to show that, while the results for silver and binary silver−gold clusters are in very favorable agreement with theoretical predictions, the published theoretical binding energy values of the molecules to gold clusters tend to consistently overestimate the experimental data, in most cases far beyond the error limits derived in the present study.

2. Experimental Section

To obtain temperature-dependent rate constants of metal cluster ion reactions with neutral reactant gases, a variable temperature rf-octopole ion trap inserted into a tandem quadrupole mass spectrometer was employed.[16,62] In brief, the noble metal cluster ions were produced by sputtering metal targets by a cold reflex discharge ion source (CORDIS).[63] Mass selection was achieved via a first quadrupole mass filter before the cluster ion beam entered the octopole ion trap. The ion trap was prefilled with about 1 Pa partial pressure of helium buffer gas and a small, well-defined fraction of reactive gases (O_2 or CO). The ion trap was attached to a helium cryostat that allowed for temperature adjustment in a range between 20 and 300 K.

The absolute pressure inside of the ion trap was measured by a Baratron gauge (MKS, Typ 627B) attached to the ion trap via a 1 mm diameter Teflon tube. For exact pressure determination inside of the ion trap, however, it has to be considered that the Baratron capacitance manometer is thermally stabilized at 318 K, in contrast to the variable temperature ion trap. Thus, the effect of thermal transpiration has to be taken into account.[64−67] This effect has been described theoretically[68,69] and experimentally[70−72] in the molecular flow pressure regime below 10^{-1} Pa. Thermal transpiration leads, in its simplest form, to a correction factor of $p_{trap}/p_{gauge} = (T_{trap}/T_{gauge})^{1/2}$, applicable to the pressure read from the gauge p_{gauge} to obtain the true trap pressure p_{trap} at trap and gauge temperatures of T_{trap} and T_{gauge},

* To whom correspondence should be addressed. Tel: +49-731-50-25455. Fax: +49-731-50-25452. E-mail: thorsten.bernhardt@uni-ulm.de.
† Universität Ulm.
‡ Freie Universität Berlin.
§ Present address: Fraunhofer-Institut für Werkstoffmechanik, Wöhlerstrasse 11, 79108 Freiburg, Germany.
⊥ Present address: Physikalisch-Technische Bundesanstalt, Abbestrasse 2-12, 10587 Berlin, Germany.

10.1021/jp810055q CCC: $40.75
Published on Web 02/27/2009

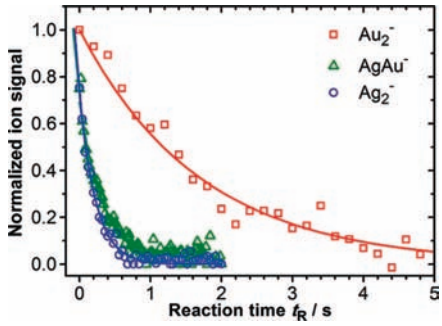

Figure 1. Experimental kinetic data of the reactions of Ag_2^-, $AgAu^-$, and Au_2^- with molecular oxygen at 300 K. The oxygen partial pressure in all three measurements amounted to 0.12 Pa. The metal cluster ion signal decays in the ion trap are plotted as a function of the reaction time t_R. The solid lines represent the fit of the integrated rate equations to the experimental data.[16]

respectively. At higher pressures corresponding to the viscous flow regime, this phenomenon is, however, not observed.[71] The present experiment operates at pressures above 1 Pa and thus just in the transition range between molecular and viscous flow. Therefore, the termolecular rate constants of the reactions studied here have been calculated employing partial pressures both with and without correction for thermal transpiration. However, the deviations in the deduced binding energies are consistently within the error bars. All reaction rate constants and binding energies presented in this contribution have been obtained with pressure correction for thermal transpiration.

At the applied pressures, thermal equilibration of the clusters with the buffer gas was achieved within a few milliseconds,[16] whereas the cluster ions were stored in the ion trap typically for 0.1 s up to some seconds. After a chosen reaction time, all ionic reactants, intermediates, and products were extracted from the ion trap, and the ion distribution was analyzed via a second quadrupole mass filter. By recording all ion intensities as a function of reaction time t_R, the rates of the reaction at a well-defined reaction temperature could be studied.

3. Data Evaluation

3.1. Theory. ***Kinetic Evaluation Procedure.*** Fitting of the integrated rate equations of a proposed reaction mechanism to these measured kinetic data by using the Detmech software[73] allows for the determination of the likelihood of the proposed reaction mechanism and for the calculation of the corresponding rate constant k of each reaction step. Figure 1 shows an example of the experimental kinetic data and the respective fitted integrated rate equations for the dimer reactions with oxygen at room temperature. For the investigated clusters, molecular oxygen adsorption is the only reaction mechanism, as confirmed by photoelectron spectroscopic measurements and theoretical simulations.[39,58,74,75] In the fitting procedure, the differential equations derived from the proposed mechanistic model are solved numerically by using the fourth-order Runge−Kutta algorithm. The optimum set of rate constants is found by a least-squares minimum search for the deviations of the measured concentrations versus the calculated ones. This method is applied to yield the simplest reaction mechanism with the best fit to the experimental data, that is, more complex mechanisms, which result in the same fit quality, are discarded.

In order to compute binding energies of the ligands to the cluster ions using the obtained rate constant k, it is necessary to consider the elementary reaction models underlying the measured processes. As an example, the generalized straightforward association reaction

$$M_n^- + X \xrightarrow{k} M_nX^- \quad (1)$$

of the negatively charged metal cluster ion M_n^- and the neutral reactant X will be examined in the following. Nevertheless, the elementary models apply to all individual reaction steps of the proposed reaction mechanism as well.

The total pressure inside of the ion trap was on the order of 1 Pa, which means that the experiments were operated in the kinetic low-pressure regime. Therefore, an elementary Lindemann-type mechanism has to be considered for reaction 1. Consequently, the reaction depends on the buffer gas pressure and becomes of third order. However, the concentrations of the reactive gas [X] and the helium buffer gas [He] in the ion trap were orders of magnitude larger than the cluster ion concentration [M_n^-], and a steady flow of the reactants was ensured. This permits the postulation of pseudo-first-order kinetics with the pseudo-first-order rate constant

$$k = k^{(3)}[\mathrm{He}][\mathrm{X}] \quad (2)$$

containing the termolecular rate constant $k^{(3)}$ as well as the buffer gas and the reactant concentration. Hence, the termolecular rate constant $k^{(3)}$ can be directly obtained from the fitted pseudo-first-order rate constant k and the partial pressures of He (p_{He}) and reactant molecules X (p_x) (X = O_2 or CO) by applying the ideal gas law to calculate the concentrations [He] and [X].

The details of reaction 1 and thus those of each reaction step of the overall proposed reaction mechanism are described by the Lindemann energy-transfer model for association reactions,[76] which is represented by the following equations

$$M_n^- + X \underset{k_d}{\overset{k_a}{\rightleftharpoons}} (M_nX^-)^* \quad (3a)$$

$$(M_nX^-)^* + He \xrightarrow{k_s} M_nX^- + He \quad (3b)$$

The reaction model includes three elementary steps, (i) the formation of an energized complex $(M_nX^-)^*$ with the rate constant k_a and (ii) the possible unimolecular decomposition back to the reactants (rate constant k_d) in competition with (iii) a stabilizing energy-transfer collision with helium buffer gas (rate constant k_s). Assuming all these elementary reaction steps to be again of pseudo-first-order and additionally employing the steady-state approximation[76] for the intermediate $(M_nX^-)^*$ leads to the overall third-order rate constant expression

$$k^{(3)} = \frac{k_a k_s}{k_d + k_s[\mathrm{He}]} \quad (4)$$

As the experiment is operating in the kinetic low-pressure regime, the decomposition rate constant can consequently be considered to be much larger than the stabilization rate constant, $k_d \gg k_s[He]$, thus simplifying the termolecular rate constant to yield

$$k^{(3)} = \frac{k_a k_s}{k_d} \quad (5)$$

The ion−molecule association rate constant k_a as well as the final stabilization rate constant k_s are well represented by ion−molecule collision rate constants as specified by Langevin theory;[77,78] k_s is only dependent on the reduced mass of the $(M_nX^-)^*$−He "scattering complex" as well as the polarizability of the helium atom. For the association reaction rate constant k_a, it is necessary to distinguish between polar (X = CO) and

TABLE 1: Measured Pseudo-First-Order (k) and Termolecular ($k^{(3)}$) Rate Constants for the Investigated Reactions of Noble Metal Cluster Anions M_n^- with Reactant Molecules X, As Well As Deduced Unimolecular Decomposition Rate Constants (k_d) of the Energized Complexes $(M_nX^-)^*$ at Various Temperatures T and the Experimental Pressure Conditions (Not Yet Corrected for Thermal Transpiration) and the Langevin Rate Constants k_a and k_s

M_n^-	X	T [K]	p(He) [Pa]	p(X) [Pa]	k [s^{-1}]	$k^{(3)}$ [10^{-28} cm^6s^{-1}]	k_a [10^{-10} cm^3s^{-1}]	k_s [10^{-10} cm^3s^{-1}]	k_d [10^9s^{-1}]
Ag^-	O_2	100	1.05	0.07	0.11 ± 0.02	0.091 ± 0.028	5.93023	5.3735	35 ± 11
		300	1.05	0.19	0.040 ± 0.002	0.036 ± 0.003	5.93023	5.3735	87 ± 7
Ag_2^-	O_2	100	1.03	≤0.01	≥39	≥230	5.57849	5.34071	≤0.013
		200	1.03	0.02	2.8 ± 1.4	16 ± 13	5.57849	5.34071	0.18 ± 0.15
		300	1.06	0.12	4.7 ± 0.4	6.7 ± 0.1	5.57849	5.34071	0.44 ± 0.05
		300	1.02	0.02	1.2 ± 0.6	11 ± 8	5.57849	5.34071	0.28 ± 0.20
$AgAu^-$	O_2	100	1.03	≤0.01	≥5	≥29	5.47002	5.32926	≤0.099
		205	1.03	≤0.01	≥1.5	≥18	5.47002	5.32926	≤0.16
		300	1.05	0.12	3.7 ± 0.3	5.3 ± 0.6	5.47002	5.32926	0.55 ± 0.06
		300	1.07	0.02	1.6 ± 0.8	14 ± 10	5.47002	5.32926	0.21 ± 0.15
Au_2^-	O_2	100	1.03	0.04	5.5 ± 0.6	8.1 ± 3.7	5.41019	5.32263	0.35 ± 0.16
		150	1.05	0.06	2.5 ± 0.4	3.6 ± 1.0	5.41019	5.32263	0.80 ± 0.22
		190	1.05	0.08	1.1 ± 0.1	1.5 ± 0.3	5.41019	5.32263	1.9 ± 0.4
		200	1.00	0.16	1.4 ± 0.1	1.0 ± 0.1	5.41019	5.32263	2.8 ± 0.3
		300	1.05	0.13	0.62 ± 0.03	0.83 ± 0.08	5.41019	5.32263	3.5 ± 0.3
	CO	100	0.96	0.24	0.64 ± 0.14	0.17 ± 0.04	6.82168	5.32286	22 ± 5
		150	1.04	0.25	0.21 ± 0.04	0.073 ± 0.015	6.72242	5.32286	49 ± 10
		200	1.04	0.25	0.11 ± 0.02	0.051 ± 0.010	6.66762	5.32286	69 ± 13
Au_3^-	CO	100	1.03	0.02	2.7 ± 1.4	7.9 ± 8.1	6.74582	5.3149	0.45 ± 0.46
		150	0.99	0.03	0.98 ± 0.33	3.0 ± 1.8	6.64766	5.3149	1.2 ± 0.7
		200	1.03	0.04	0.15 ± 0.04	0.44 ± 0.18	6.59347	5.3149	7.9 ± 3.3
Ag_3^-	O_2	95	1.03	0.06	1.8 ± 0.3	1.7 ± 0.6	5.45621	5.32775	1.7 ± 0.6
		200	1.07	0.14	0.53 ± 0.04	0.43 ± 0.05	5.45621	5.32775	6.8 ± 0.8
		300	1.02	0.23	0.076 ± 0.004	0.059 ± 0.004	5.45621	5.32775	49 ± 3
Ag_4^-	O_2	300	1.04	≤0.01	≥100	≥600	5.39403	5.3208	≤0.0048
Ag_5^-	O_2	200	1.06	≤0.01	≥4.4	≥50	5.35637	5.31647	≤0.057
		300	1.04	0.09	1.3 ± 0.2	2.5 ± 0.5	5.35637	5.31647	1.1 ± 0.2

nonpolar ($X = O_2$) reactants. In the case of nonpolar molecules, the simple Langevin rate constant can be used as well, while for polar reactants, the Langevin rate constant must be corrected by an empirical expression found by Su et al.[79] that contains the permanent dipole moment of X. According to Langevin theory, ion−molecule reactions are basically interactions between a charge and an induced dipole and thus exhibit no activation barrier and hence no temperature dependence.[80] Therefore, any observed cluster size and temperature dependence must be contained in the unimolecular decomposition rate constant k_d.

Applying eqs 2 and 5 allows for the determination of an experimental unimolecular decomposition rate constant k_d, which is listed in Table 1 for all investigated reactions together with k, $k^{(3)}$, k_a, and k_s and the experimental conditions. The k_d is also well represented by statistical unimolecular reaction rate theory in the framework of the RRKM (Rice−Ramsperger−Kassel−Marcus) model.[81] This theory is usually applied to determine k_d from the known binding energy between the adsorbed ligand and the cluster ion. In our experimental approach, k_d is the measured quantity which consequently allows for the determination of the binding energy. In order to understand the assumptions made and the possible sources of error discussed in the following sections, it is necessary to briefly outline the concepts of RRKM theory that are important to our analysis.

RRKM Theory. RRKM theory[81,82] describes the unimolecular decomposition rate constant k_d as defined in eq 3a using statistical mechanics. Thereby, the decomposition reaction step is considered to proceed via

$$(M_nX^-)^* \xrightarrow{k_d} (M_nX^-)^{\ddagger} \rightarrow M_n^- + X \qquad (6)$$

involving the transition state (TS) $(M_nX^-)^{\ddagger}$. In RRKM theory, it is important to distinguish between the energized complex $(M_nX^-)^*$ and the TS $(M_nX^-)^{\ddagger}$. While the TS $(M_nX^-)^{\ddagger}$ describes an intermediate between reactants and products, the energized complex $(M_nX^-)^*$ is a complex M_nX^- which contains a total nonfixed energy $E^* \geq E_0$ in its active degrees of freedom. E_0 denotes the critical energy which is necessary for the reaction to occur and which is assumed to be equal to the bond dissociation energy or the binding energy, respectively. Any energy that can be redistributed between the various degrees of freedom of the complex is called nonfixed, while fixed energy (e.g., zero-point energy, translational energy, and adiabatic vibrations and rotations) cannot be redistributed and thus is not considered in the theory. The total energy E^* of the complex $(M_nX^-)^*$ can be expressed as the sum of (i) the potential energy E_0 gained in forming the complex, (ii) the vibrational energy of the reactants, which is the vibrational energy of the cluster $E_{vib}(M_n^-)$ before reaction as the molecules $X = O_2$, CO can be considered vibrationally cold at the investigated reaction temperatures, and (iii) the energy E_{free} contained in the translational and rotational degrees of freedom which is converted into internal energy of $(M_nX^-)^*$ upon reaction of M_n^- with X.[83]

The RRKM decomposition rate constant is given by

$$k_d^{RRKM}(E^*) = L^{\ddagger}\frac{W(E_{vr}^{\ddagger})}{h\rho(E^*)} \qquad (7)$$

wherein $L^{\ddagger}$ denotes the reaction path degeneracy, $W(E_{vr}^{\ddagger})$ the sum of vibrational−rotational quantum states of the TS, $\rho(E^*)$ the density of quantum states of the energized complex, and h is Planck's constant. Note that, since the total nonfixed energy E^* can be expressed as $E^* = E_0 + E_{vib}(M_n^-) + E_{free}$ and both $E_{vib}(M_n^-)$ and E_{free} are functions of the reaction temperature T, the expression $k_d^{RRKM}(E^*)$ is equivalent to $k_d^{RRKM}(T)$.

A further, more subtle problem with respect to the total available energy is posed by the adiabatic rotational degrees of freedom, which have not been considered so far. Adiabatic

TABLE 2: Calculated and Approximated Frequencies for the Energized Complexes $(M_nX^-)^*$ and the "Loose" TS $(M_nX^-)^‡$

	$(M_nX^-)^*$	$(M_nX^-)^‡$ ("loose" TS)
M_nX^-	vibrational frequencies [cm^{-1}]	vibrational frequencies [cm^{-1}]
AgO_2^-	416; 1205; 127[a]	1580; 64
$Ag_2O_2^-$	145;[b] 399; 1205; 69, 100, 258	145; 1580; 35, 50, 129
$AgAuO_2^-$	138;[c] 399; 1205; 69, 100, 258	138; 1580; 35, 50, 129
$Au_2O_2^-$	127; 416; 1205; 69, 100, 258[a] (139; 414; 1186; 37, 44, 226)[d]	127; 1580; 35, 50, 129 (139; 1580; 19, 22, 113)
Au_2CO^-	127; 375; 1856; 47, 69, 258[a]	127; 2170; 24, 35, 129
Au_3CO^-	25, 31, 101, 165; 358; 2031; 58, 212, 263[a]	25, 31, 101, 165; 2170; 29, 106, 132
$Ag_3O_2^-$	129, 104, 83, 83;[b] 221; 1205; 50, 50, 50	129, 104, 83, 83; 1580; 25, 25, 25
$Ag_4O_2^-$	131, 113, 91, 90, 72, 72;[b] 370; 1205; 50, 50, 50, 50	131, 113, 91, 90, 72, 72; 1580; 25, 25, 25, 25
$Ag_5O_2^-$	132, 119, 103, 83, 94, 82, 82, 66, 66;[b] 271; 1205; 50, 50, 50, 50	132, 119, 103, 83, 94, 82, 82, 66, 66; 1580; 25, 25, 25, 25

[a] Ref 86. [b] Ref 87. [c] Ref 89. [d] Ref 44.

rotations are those for which the angular momenta and thus the quantum states stay constant during the conversion of $(M_nX^-)^*$ to $(M_nX^-)^‡$. However, when the geometry and, with it, the moment of inertia changes, additional energy is released into other degrees of freedom and is contained in the energy of the transition state ($E_{vib}(M_n^-) + E_{free}$). Hence, $E^* = E_0 + E_{vib}(M_n^-) + E_{free}$ does not reflect the actually available total energy of the complex $(M_nX^-)^*$ which has to be rather denoted as $E^*_{act} < E^*$. Neglecting adiabatic rotations in the evaluation procedure therefore would result in too low of a value for the binding energy. The treatment of adiabatic rotations as well as the energized molecule and the TS are detailed in the next sections.

3.2. Fitting Procedure. ***MassKinetics Input.*** In this contribution, RRKM decomposition rate constants k_d and thus binding energies E_0 are calculated using the software package *MassKinetics* developed by Drahos et al.[84] This computer algorithm applies the harmonic oscillator model with internal rotations approximated by low-frequency vibrations. The density and sum of states of eq 7 are calculated by direct count using the Beyer−Swinehart algorithm.[82] Furthermore, adiabatic rotations are taken into account by expressing them as a "rotational barrier" E_{RB}, that is, a correction factor to the too low binding energy and the too high available energy E^* that would have been obtained by neglecting adiabatic rotations (see discussion above).[84]

To calculate the decomposition rate constant k_d according to eq 7, *MassKinetics* requires the specification of the following parameters: (i) the mass of the energized complex $(M_nX^-)^*$, (ii) the critical energy for dissociation (binding energy) E_0, (iii) the actual total nonfixed energy E^*_{act}, (iv) the "rotational barrier" E_{RB}, and (v) the reaction path degeneracy $L^‡$. The mass is given by the stoichiometry of the reaction product $(M_nX^-)^*$, the critical energy E_0 is the quantity in demand, and the actual nonfixed total energy E^*_{act} is calculated according to $E^*_{act} = E^* - E_{RB} = E_0 + E_{vib}(M_n^-) + E_{free} - E_{RB}$.[82,83] For metal cluster reactions with one adsorbed ligand, the reaction path degeneracy is $L^‡ = 1$. Adiabatic rotations are considered in the following calculations by approximating E_{RB} according to the formula[82,85]

$$E_{RB} = \left(\frac{r_c^2}{r_e^2} - 1\right) k_B T \qquad (8)$$

where r_c denotes the M_n-X^- distance in the transition state represented by the capture radius of the long-range potential between M_n^- and X and r_e denotes the M_n-X^- distance of the energized molecule represented by the equilibrium radius. The effect of the temperature dependence of E_{RB} on the resulting binding energy E_0 is negligible. Therefore, a fixed mean E_{RB} value at $T = 200$ K is employed for the fitting procedure. Additionally, the energized molecule $(M_nX^-)^*$ and the TS $(M_nX^-)^‡$ are each characterized by its normal frequencies. While for $(M_nX^-)^*$ vibrational frequencies can be obtained by DFT calculations or simple approximations, the TS is usually unknown, and several assumptions are necessary.

Energized Molecule and Transition-State Models. For the complexes $(AgO_2^-)^*$, $(Au_2O_2^-)^*$, $(Au_2CO^-)^*$, and $(Au_3CO^-)^*$, the normal frequencies have been calculated by Bonačić-Koutecký et al. using ab initio theory.[86] The vibrational frequencies of $(Ag_nO_2^-)^*$ ($n = 2-5$) and $(AgAuO_2^-)^*$ are not available and therefore have been estimated here. The metal−metal vibrations of Ag_n^- are adopted from Spasov et al.[87] using the elastic theory of bulk materials,[88] and the theoretical value for the Ag−Au frequency has been reported to be 138 cm^{-1}.[89] The computed O−O vibrations for AgO_2^- and $Au_2O_2^-$ amount to 1205 cm^{-1},[86] which is also adopted for $(Ag_nO_2^-)^*$ and $(AgAuO_2^-)^*$. The $Ag_n-O_2^-$ stretching frequencies are estimated by modeling the potential along the reaction coordinate by a Morse function and assuming a constant Morse parameter α for all cluster sizes as well as for O_2 on bulk silver.[90] Introducing the theoretical binding energies of O_2 to Ag_n^- (1.12, 0.36, 0.96, and 0.53 eV for $n = 2-5$)[58] and O_2 to bulk silver (0.47 eV)[91,92] as well as the vibrational frequency of the O_2 bond to bulk silver (241 cm^{-1})[93,94] yields the desired frequencies for all cluster sizes. Since the $Ag_n-O_2^-$ and $Au_n-O_2^-$ stretching frequencies are similar and since in the binary complex $(AgAuO_2^-)^*$ the oxygen molecule is most probably bound to the silver atom,[39] the same stretching frequency as that for the pure silver dimer oxide is assumed for $AgAu-O_2^-$. Further unknown vibrations must be low-frequency bending modes. For $(Au_2O_2^-)^*$, these extra vibrations have been theoretically evaluated to amount to 69, 100, and 258 cm^{-1}.[86] These values are also adopted for the dimers $(Ag_2O_2^-)^*$ and $(AgAuO_2^-)^*$. For the remaining silver−oxygen complexes, these frequencies are chosen to be 50 cm^{-1}. All frequencies used to compute the dissociation energies are summarized in Table 2.

While for numerous energized complexes DFT calculations are available or simple estimates are possible, the transition state is usually unknown, and reasonable assumptions are necessary. In the following, the bond dissociation energy E_0 for each complex $(M_nX^-)^*$ is calculated by employing two different transition-state models, a "tight" TS and a more realistic "loose" TS. The "tight" transition state, which is usually associated with rearrangement processes, has the same vibrational modes as the energized molecule, less one. This particular one is treated as internal translation along the reaction coordinate. This model represents the tightest reasonable transition state and gives a lower limit for the dissociation energy.[95] No "rotational barrier" exists for a "tight" TS ($E_{RB} = 0$).

In contrast, the "loose" TS, common to simple bond cleavage reactions, not only has one vibration removed and transformed into internal translation along the reaction coordinate but, in addition, also has the low-frequency bending vibrations scaled by a factor of $f < 1$.[96] Thus, the TS can be tuned to be "tight" (lower limit for E_0) or "loose" (upper limit for E_0) by varying this factor. A convenient measure of the "looseness" of a TS is the entropy of activation $S^{\ddagger}$ calculated from the vibrational frequencies of the energized complex and of the TS. Values of $S^{\ddagger} \leq 0$ are indicative of a tight transition state, while values of $S^{\ddagger} \geq 0$ indicate a loose transition state.[96] Commonly, the bending vibrations are scaled by $f = 0.5$,[87,97] which is also applied for all TSs under investigation here and leads to $S^{\ddagger} > 0$.

Error Analysis. To obtain the error limits of the binding energy values determined here and thus to assess their accuracy, (i) the uncertainties of the measured kinetic data and (ii) the uncertainties in the description of $(M_nX^-)^*$ and $(M_nX^-)^{\ddagger}$ have to be considered.

(i) As evaluative quantities, the error bars of the measured k_d values include uncertainties in the fitting procedure to obtain k (cf. Figure 1 and the Kinetic Evaluation Procedure section) and errors in the measured gas pressure, which are considered to be ± 0.01 Pa according to the detection limit of the Baratron gauge.

(ii) The determination of the energized complex's vibrational frequencies as described above is a rough approximation; however, not the exact frequencies but the distribution of frequencies is crucial. Especially the low-frequency bending modes that have been assumed to be 50 cm^{-1} for $(Ag_nO_2^-)^*$ ($n = 3-5$) are immaterial as only their change on the way to the transition state is relevant to the decomposition rate constant.[88] To demonstrate that the absolute accuracy of vibrational frequencies is not essential, the binding energy has been calculated for two different sets of $(Au_2O_2^-)^*$ vibrational frequencies reported by Bonačić-Koutecký et al.[86] and by Ding et al.[44] (cf. also Table 2). The deduced binding energies are 0.93 ± 0.10 and 0.86 ± 0.10 eV, respectively, agreeing completely within the error limits.

In contrast, the cluster−ligand vibration, representing the reaction coordinate, is removed in the TS, and thus, the exact frequency of this vibration has more influence on the bond dissociation energy. However, as an example, it can be shown for $(Au_2O_2^-)^*$ that even a significant change of this frequency from 416 to 216 cm^{-1} only shifts the binding energy from 0.93 ± 0.10 to 0.82 ± 0.10 eV, which lies well within the error limits. The error in approximating the reaction coordinate frequency from the Morse potential as described above is considerably smaller than the one assumed in this example. Of more importance to the resulting binding energies is the selection of the TS configuration ("tight" or "loose"), as can be seen from the calculated values given in Tables 3 and 4.

Furthermore, the total nonfixed energy E^*_{act} is determined from $E_{vib}(M_n^-)$ and E_{free}. In this calculation, E_{free} is assumed to amount to $1/2k_BT$ for each translational and rotational degree of freedom that is lost by forming the complex $(M_nX^-)^*$ and is thus converted into internal energy. Additionally, $E_{vib}(M_n^-)$ contributes k_BT for each vibrational degree of freedom. These values represent the classical limit and are thus certainly upper limits at the low to moderate reaction temperatures of our experiment.[90]

To summarize, since "tight" TSs are usually associated with rearrangement processes and "loose" TSs are common for simple cleavage reactions, the "tight" TS model clearly represents a lower limit for the dissociation energy in the evaluation procedure described above. In contrast, the consideration of thermal transpiration (cf. Experimental Section) and the rotational barrier E_{RB} as well as applying the upper classical limit for the determination of $E_{vib}(M_n^-)$ represent positive contributions to the obtained binding energies of the "loose" TS. Thus, the presented binding energies of the "loose" TSs correspond to an upper limit which can only be further increased by reducing the scaling factor f and hence making the TS even "looser".

To illustrate the accuracy of the k_d fitting procedure employed to determine the binding energies, Figure 2 displays the experimentally obtained reaction-temperature-dependent decomposition rate constants together with the calculated RRKM $k_d(T)$ curves for both "tight" and "loose" TSs for all investigated complexes. In addition to the best-fit RRKM $k_d(T)$ curves determining the binding energy E_0, also error limits of the binding energies have been estimated by varying E_0 to include all experimental k_d values. These uncertainties of E_0 do not, of course, account for possible deficiencies in the TS models or the RRKM model itself. Only in the case of $Ag_4O_2^-$, where only one k_d value was obtained experimentally (representing an upper limit), could no binding energy error limits be

TABLE 3: Binding Energies of O_2 to All Investigated Cluster Ions M_n^- As Deduced by Employing RRKM Theory for "Tight" and "Loose" TSs in Comparison with Theoretical Literature Values[a]

M_n^-	E_0 [eV] "tight" TS	E_0 [eV] "loose" TS	theoretical E_0 [eV]
Ag^-	+	+	0.36[b]
Au^-	−	−	0.18,[c] 0.22,[d] 0.52,[e] 1.04[f]
Ag_2^-	1.10 ± 0.10	1.64 ± 0.20	1.12[b]
$AgAu^-$	1.10 ± 0.15	1.59 ± 0.20	0.94[g]
Au_2^-	0.60 ± 0.10	0.93 ± 0.10	0.95,[d] 1.06,[h] 1.07,[i] 1.08,[c] 1.25,[f] 1.39[j]
Ag_3^-	0.18 ± 0.04	0.37 ± 0.05	0.36[b]
Ag_2Au^-	−	−	−
$AgAu_2^-$	−	−	−
Au_3^-	−	−	0.015,[h] 0.03,[c] 0.04,[d] 0.46,[k] 0.50[l]
Ag_4^-	≥ 0.84	≥ 1.23	0.96[b]
Ag_5^-	0.34 ± 0.04	0.57 ± 0.03	0.53[b]

[a] A "+" indicates that no binding energy determination was possible via RRKM analysis, although a reaction product has been observed experimentally. A dash indicates that no adsorption products of O_2 to this cluster were detected under our experimental conditions. [b] Ref 58. [c] Ref 46. [d] Ref 44. [e] Ref 34. [f] Ref 74. [g] Ref 39. [h] Ref 102. [i] Refs 41 and 42. [j] Ref 33. [k] Ref 40. [l] Ref 110.

TABLE 4: Binding Energies of CO to All Investigated Cluster Ions M_n^- As Deduced by Employing RRKM Theory for "Tight" and "Loose" TSs in Comparison with Theoretical Literature Values[a]

M_n^-	E_0 [eV] "tight" TS	E_0 [eV] "loose" TS	theoretical E_0 [eV]
Ag^-	−	−	−
Au^-	−	−	0.085,[b] 0.46[c]
Ag_2^-	−	−	−
$AgAu^-$	−	−	−
Au_2^-	0.18 ± 0.02	0.38 ± 0.04	0.34,[b] 0.77,[d] 0.78,[c] 0.96,[e] 0.97,[f]
Ag_3^-	−	−	−
Ag_2Au^-	−	−	−
$AgAu_2^-$	−	−	−
Au_3^-	0.28 ± 0.04	0.46 ± 0.05	0.76,[c] 0.96[f]
Ag_4^-	−	−	−
Ag_5^-	−	−	−

[a] A dash indicates that no adsorption products of CO to this cluster were detected under our experimental conditions. [b] Ref 55. [c] Ref 38. [d] Ref 30. [e] Ref 33. [f] Ref 110.

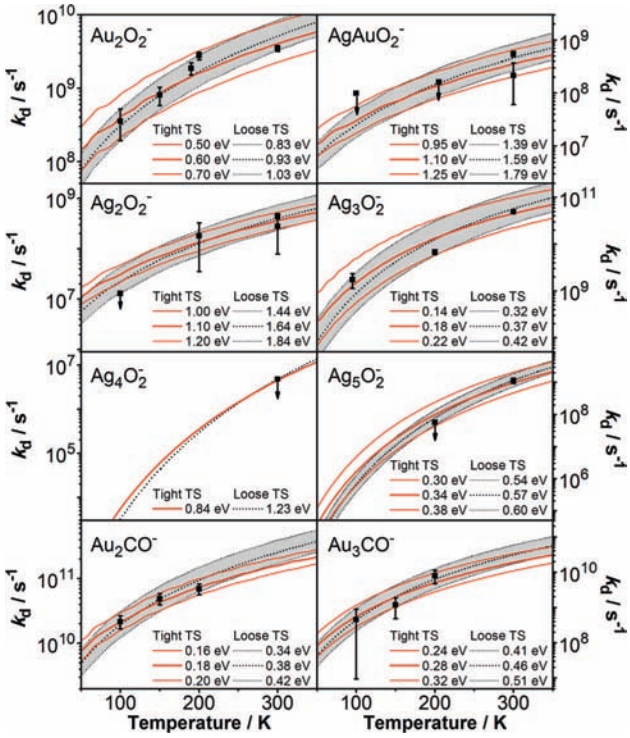

Figure 2. Experimental and RRKM decomposition rate constants k_d as a function of temperature. Solid squares represent the experimentally obtained temperature-dependent decomposition rate constants k_d. Arrows indicate that the values reflect upper limits (cf. Table 1). Red solid lines represent RRKM $k_d(T)$ curves computed for different dissociation energies E_0 for a "tight" transition state. Shown are the best fit to the experimental data (thick line) and estimated upper and lower binding energy limits (thin solid lines). Black dotted lines represent RRKM $k_d(T)$ curves computed for different dissociation energies E_0 for a "loose" transition state. Shown are the best fit to the experimental data (thick dotted line) and estimated upper and lower binding energy limits (thin dotted lines, shaded area). The wiggles apparent in some of the RRKM $k_d(T)$ curves are due to the stepwise calculation procedure required by the software and do not relate to a physical origin.

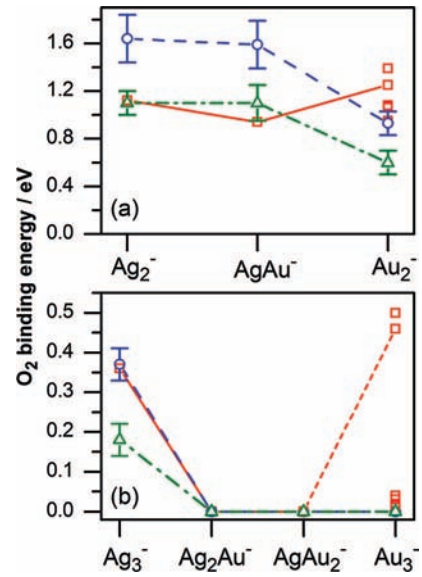

Figure 3. Composition-dependent binding energies of O_2 to (a) $Ag_nAu_{2-n}^-$ ($n = 0-2$) and (b) $Ag_nAu_{3-n}^-$ ($n = 0-3$). Red squares/solid and short dashed line: Theoretical literature data (cf. Table 3). Blue circles/dashed line: Binding energies determined by assuming a "loose" TS. Green triangles/dash−dotted line: Binding energies determined by assuming a "tight" TS. The lines are drawn to guide the eye.

estimated. All thus-obtained binding energies E_0 are listed in Tables 3 and 4.

4. Results and Discussion

4.1. O_2 Adsorption. The determined O_2 binding energies for both "tight" and "loose" TSs together with the available theoretical literature values are summarized in Table 3.

4.1.1. Composition Dependence. *Monomers Ag⁻, Au⁻.* Among the atomic ions, Au^- and Ag^-, only the silver atom reacts with molecular oxygen. Yet, subsequent to the adsorption of a first O_2 molecule, the sequential adsorption of a second oxygen molecule resulting in the product AgO_4^- proceeds so fast that the intermediate AgO_2^- cannot be detected on the time scale of our experiment.[16,58] Nevertheless, the adsorption of the first oxygen molecule represents the rate-determining step. Thus, the fitted rate constant corresponds to the formation of AgO_2^-. However, due to the small number of vibrational degrees of freedom, RRKM theory fails to fit the experimental k_d values, and it is thus not possible to evaluate the binding energy of O_2 to Ag^-. The reported theoretically obtained value amounts to 0.36 eV.[58]

Dimers $Ag_nAu_{2-n}^-$ ($n = 0, 1, 2$). In agreement with previous investigations reported in the literature,[20,74,98−101] the dimer anions Ag_2^-, $AgAu^-$, and Au_2^- were found to adsorb one oxygen molecule each.[16,58,61] The observation of products containing only O_2 and no single oxygen atom as well as photoelectron spectroscopic measurements on $Ag_2O_2^-$ [75] and $Au_2O_2^-$ [74] lead to the conclusion that oxygen is bound molecularly to the dimer anions. The reaction kinetics of the dimer anions with O_2 at 300 K are shown in Figure 1. RRKM analysis of the experimentally obtained temperature-dependent decomposition rate constants k_d yields the corresponding binding energies $E_0(Ag_2O_2^-) = 1.10 \pm 0.10$ eV, $E_0(AgAuO_2^-) = 1.10 \pm 0.15$ eV, and $E_0(Au_2O_2^-) = 0.60 \pm 0.10$ eV for a "tight" TS and $E_0(Ag_2O_2^-) = 1.64 \pm 0.20$ eV, $E_0(AgAuO_2^-) = 1.59 \pm 0.20$ eV, and $E_0(Au_2O_2^-) = 0.93 \pm 0.10$ eV for a "loose" TS. Apparently, the highest binding energy is obtained for the pure silver cluster, and it decreases with increasing gold content. However, the substitution of one silver atom for one gold atom appears to change the O_2 binding energy only slightly.

These composition-dependent binding energies E_0 for "tight" and "loose" TSs are compared in Table 3 and in Figure 3a to theoretically obtained values from the literature. For the silver dimer ($Ag_2O_2^-$) and the binary dimer ($AgAuO_2^-$), the experimental binding energies obtained using a "loose" TS assumption are considerably higher than the theoretical data. Employing a "tight" TS for $Ag_2O_2^-$ results in a binding energy agreeing very well with the reported theoretical value of 1.12 eV.[58] For $AgAuO_2^-$, there are two different theoretical binding energies depending on the adsorption site of O_2. Since the gold atom in $AgAu^-$ is more electronegative than the silver atom, the binding of the electron-accepting oxygen molecule to the gold atom is less favorable than that to the silver atom. The calculated dissociation energies are 0.33 and 0.94 eV for the gold and the silver atom, respectively.[39] The latter value agrees well with the RRKM energy for a "tight" TS. The phenomenon of a better agreement between experiment and theory for the dimer using a "tight" TS was previously observed for the CO adsorption on Cu_2^+.[90] However, the large discrepancy between the theoretical data and the experimentally obtained RRKM dissociation energies for a "loose" TS can also be easily removed by

changing the scaling factor for the bending modes from $f = 0.5$ to 0.8, which means by making the TS a little "tighter". This yields $E_0(Ag_2O_2^-) = 1.2 \pm 0.1$ eV and $E_0(AgAuO_2^-) = 1.16 \pm 0.15$ eV, also well in accord with the theoretical data.

In contrast to $Ag_2O_2^-$ and $AgAuO_2^-$, both limiting RRKM binding energies for $Au_2O_2^-$ are clearly below the reported theoretical values that range from 0.95 to 1.39 eV.[33,41,42,44,46,74,102] The only previously reported experimental value for the binding energy of O_2 to Au_2^- had been obtained via collision-induced dissociation (CID) and amounts to 1.01 ± 0.14 eV.[27] Because of the CID methodology employed to obtain this value, it represents an upper limit for the binding energy[103] and thus is in good agreement with our experimental values.

From Figure 2a, it is apparent that, whereas the theoretical data predict higher binding energies of oxygen to the gold dimer compared to the other two dimers, the experimental trend is clearly opposite. However, the experimentally observed binding energies of this work are in accord with the composition-dependent trend in the measured vertical detachment energies (VDE) of the dimers. The VDE is a measure of the energetic location of the highest occupied molecular orbital (HOMO) and provides insight into the ability of electron donation to a potential ligand molecule. Since molecular oxygen is an electron acceptor, the VDE is inversely related to the binding energy of molecular oxygen.[100,101] A low VDE promotes a facile electron transfer to the O_2 $2p\pi^*$ orbital and thus results in a strong $Ag_nAu_{2-n}-O_2^-$ bond. The measured VDEs of the dimers increase with increasing gold content (Ag_2^-: 1.06[104] and 1.1 eV;[105] $AgAu^-$: 1.43 eV;[106] and Au_2^-: 2.01 eV[104,107,108]). The particularly high VDEs of gold clusters with respect to those of silver is due to the relativistic contraction of the gold s orbitals and therefore supports the composition-dependent trend of the O_2 binding energy as measured in our experiments.

Trimers $Ag_nAu_{3-n}^-$ (n = 0, 1, 2, 3). The composition dependence of the reactivity toward oxygen is even more pronounced in the case of the trimer anions, as shown in Figure 3b. While Au_3^- and both binary silver−gold clusters $AgAu_2^-$ and Ag_2Au^- do not react with molecular oxygen,[16] Ag_3^- readily adsorbs two oxygen molecules, forming $Ag_3O_4^-$.[58,61] As in the case of the monomer, the intermediate $Ag_3O_2^-$ cannot be detected on the time scale of our experiment, and thus, the adsorption of the first oxygen molecule represents the rate-determining step. The missing reactivity of the other trimers is in accord with the high VDEs of Au_3^- (3.5−3.89 eV[104,107−109]), $AgAu_2^-$ (3.86 eV[106]), and Ag_2Au^- (2.97 eV[106]). Even the silver trimer exhibits a comparably high VDE of 2.43 eV,[104,105] implying a rather low binding energy to O_2. Indeed, the RRKM analysis of the experimentally obtained decomposition rates yields small dissociation energies of only 0.18 ± 0.04 and 0.37 ± 0.05 eV for a "tight" and a "loose" TS, respectively. The theoretically calculated value of 0.36 eV[58] is in excellent agreement with the experimental value for a "loose" TS model. No theoretical data have been reported for the binding of O_2 to the mixed trimers. It is however interesting to note that for Au_3^-, the reported theoretical binding energy values span a wide range from 0.015 to 0.50 eV[40,44,46,102,110] (cf. Table 3).

To summarize, in contrast to the dimers $Ag_nAu_{2-n}^-$ ($n = 0-2$), where the substitution of one silver atom by one gold atom does not significantly change the reaction behavior, the trimers $Ag_nAu_{3-n}^-$ ($n = 0-3$) become completely unreactive toward O_2 by the mere exchange of one single silver atom.

4.1.2. Size Dependence. *Silver Anions Ag_n^- (n = 1−5).* As indicated above, the reaction of small silver anions Ag_n^- ($n = 1-5$) with molecular oxygen bears an interesting size-dependent product alternation. All cluster sizes with an even number n of silver atoms adsorb one O_2, while all odd n cluster sizes adsorb up to two oxygen molecules. An exception is Ag_4^-, which at first only forms $Ag_4O_2^-$ at 300 K and short reaction time but then further reacts with two extra O_2 molecules, yielding $Ag_4O_6^-$.[58] No products with an odd number of oxygen atoms are detected.[16,25,58] As already outlined, for Ag^-, Ag_3^-, and Ag_5^-, the intermediate products $Ag_nO_2^-$ are not observed, which leads to the conclusion that the adsorption of the first O_2 is the rate-determining step in the overall reaction. In any case, the measured rate constants for the reactions of the even size silver clusters are always considerably larger than those of the odd size clusters (cf. Table 1).

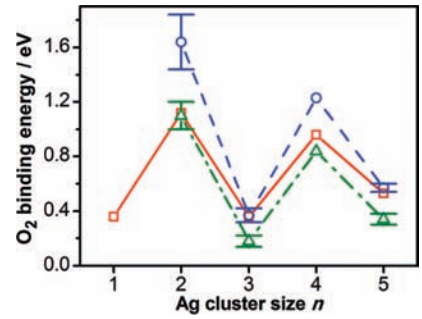

Figure 4. Cluster-size-dependent binding energies of O_2 to Ag_n^- ($n = 1-5$). Red squares/solid line: Theoretical literature data.[58] Blue circles/dashed line: Binding energies determined by assuming a "loose" TS. Green triangles/dash−dotted lines: Binding energies determined by assuming a "tight" TS. The lines are drawn to guide the eye.

This pronounced odd−even alternation in the reactivity of Ag_n^- ($n = 1-5$) toward molecular oxygen can be attributed to the alternating paired and unpaired 5s electrons of Ag_n^- with cluster size[25] and is in agreement with the alternating vertical detachment energies for Ag_2^- (1.06[104] and 1.10 eV[105]), Ag_3^- (2.43 eV[104,105]), Ag_4^- (1.63[105] and 1.65 eV[104]), and Ag_5^- (2.11[104] and 2.12 eV[105]).

Figure 4 displays the binding energies versus cluster size for a first oxygen molecule adsorbed on Ag_n^- ($n = 1-5$) obtained from RRKM calculations for "tight" and "loose" TSs in comparison with the theoretically predicted values.[58] The data are also listed in Table 3. Note that for $Ag_4O_2^-$, only a lower limit of the rate constant k and thus an upper limit for k_d could be estimated from the ion mass distribution recorded at 300 K since the reaction proceeds too fast to be resolved on the time scale of our experiment.

The determined RRKM binding energies reflect the distinct odd−even alternation of the observed reactivity of Ag_n^- toward O_2. Whereas all values obtained by using a "tight" TS are either in good agreement or slightly below the theoretical energies, the "'loose" TS model yields different trends for odd and even n cluster sizes. While for the weakly bonding odd n clusters, Ag_3^- and Ag_5^-, the RRKM binding energies ("loose" TS) are in excellent agreement with the theoretical values, the evaluated E_0 for the stronger-binding even n clusters, Ag_2^- and Ag_4^-, are somewhat larger than the theoretically predicted values (cf. Figure 4). This implicates that for the stronger binding complexes, the chosen TS model with $f = 0.5$ is slightly too "loose" and thus might overestimate the binding energies. Nevertheless, for all investigated Ag_n^- cluster sizes, the deduced RRKM O_2 binding energy values are in very favorable agreement with the available theoretical data.

4.2. CO Adsorption. In accord with previous measurements,[98] all investigated silver anions Ag_n^- ($n = 1-5$)[16,25,61] as well as the binary silver−gold clusters $Ag_nAu_m^-$ ($n + m = 2$,

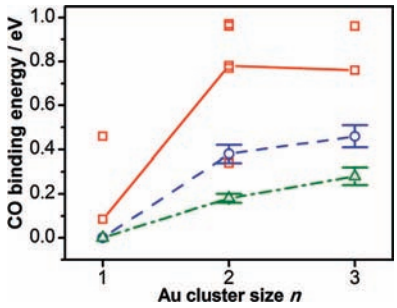

Figure 5. Cluster-size-dependent binding energies of CO to Au_n^- ($n = 1-3$). Red squares/solid line: theoretical literature data (cf. Table 4). Blue circles/dashed line: Binding energies determined assuming a "loose" TS. Green triangles/dash−dotted line: Binding energies determined assuming a "tight" TS. The lines are drawn to guide the eye.

3)[16] are found to be unreactive toward carbon monoxide over the whole accessible temperature range from 100 to 300 K. This has been previously attributed to the large s−d valence level splitting in silver compared to, for example, gold, which renders bonding of CO to metals unfavorable in the framework of the Blyholder model.[111−113] However, the gold cluster anions, Au_n^- ($n = 1-3$) do also not react with CO at room temperature.[29,114,115] Only at ion trap temperatures below 250 K are Au_2^- and Au_3^- observed to adsorb one CO molecule each. At an even lower temperature of 100 K, additional products $Au_2(CO)_2^-$ and $Au_3(CO)_2^-$ are detected, while Au^- still remains unreactive. Furthermore, kinetic measurements reveal that the dimer adsorption products Au_2CO^- and $Au_2(CO)_2^-$ reach an equilibrium at long reaction times, whereas Au_3CO^- almost completely reacts further to $Au_3(CO)_2^-$.[29] These observations are reflected in the measured rate constant k of the first CO adsorption, which increases with cluster size from Au^- to Au_3^-, as can be seen from Table 1. This increase in k has been discussed previously in terms of the onset of the internal vibrational energy redistribution with the transition from the dimer to the trimer.[29,90]

The deduced RRKM binding energies for "tight" and "loose" TSs are listed in Table 4 and are plotted together with the available theoretical literature values in Figure 5. Our RRKM binding energies are always below 0.5 eV, suggesting rather weak interactions. This is in good agreement with a previous rough estimation based on gas-phase reaction kinetics and RRK considerations, which gave an average value for the CO binding energy to Au_2^- and Au_3^- of $E_0 = 0.5$ eV.[29] A binding energy of CO to Au_2^- of 0.91 eV was deduced previously from the femtosecond dissociation time constant in combination with statistical RRK analysis.[30] This is a considerably higher binding energy value than the one resulting from our RRKM analysis. The same publication also reports the result of an ab initio calculation resulting in a lower binding energy of 0.77 eV.[30]

Still, as can be seen from Table 4 and Figure 5, all theoretically predicted E_0 values for the CO binding to Au_3^- are considerably higher than our experimental RRKM data, far off of the estimated error limits. Also for Au_2^-, all but one theoretical value are much larger than the RRKM E_0 limits of the "tight" and "loose" TS models. Solely, one theoretical literature value (0.34 eV[55]) coincides favorably with the "loose" TS RRKM binding energy of 0.38 ± 0.04 eV. This might be likely due to the fact that DFT calculations, which have been employed to obtain most of the binding energies, tend to overestimate the binding to gold clusters, whereas the (more than 0.3 eV lower) value coinciding with the "loose" TS RRKM binding energy was the result of a accurate wave-function-based coupled cluster method.[55]

As noted above already for the adsorption of molecular oxygen, also in the case of the CO adsorption to the small anionic gold clusters, a pronounced deviation is observed between almost all theoretical literature values and the experimental CO binding energies reported here. Generally, the experimental E_0 data obtained in the present contribution are more than 0.3 eV lower than the theoretical data.

5. Conclusion

In this contribution, RRKM theory was employed to extract reliable experimental binding energies of O_2 and CO to small noble metal cluster anions from temperature-dependent kinetic data. The underlying models and possible sources of error were therefore discussed in detail. Binding energies of molecular oxygen and carbon monoxide to Au_n^- ($n = 1-3$), Ag_n^- ($n = 1-5$), and $Ag_nAu_m^-$ ($n + m = 2, 3$) clusters were determined using two different transition-state models. Employing a "tight" TS, the obtained RRKM binding energies are smaller than the corresponding theoretical ab initio values for almost all investigated reactive systems (except $AgAu^-$). This result supports the consistency of the molecular models and is to be expected since, for simple bond cleavage reactions, a "tight" TS clearly yields the lower-limit dissociation energies.[95] In contrast, assuming a "loose" transition state by scaling the low-frequency bending modes by a factor of $f = 0.5$ results in two different trends. The deduced binding energies of the weakly binding complexes $Ag_3O_2^-$ and $Ag_5O_2^-$ agree well with theoretical data. However, binding energies of the stronger binding complexes $AgAuO_2^-$, $Ag_2O_2^-$, and $Ag_4O_2^-$ are considerably larger than the theoretically obtained data. This discrepancy is removed if the frequency scaling factor is enhanced from $f = 0.5$ to 0.8, which means by making the TS "tighter". For this reason, the comparison to the theoretical literature data in these cases might lead to the conclusion that for the stronger binding complexes, the chosen "loose" TS model tends to overestimate the bond dissociation energy.

However, the situation completely changes if the pure gold clusters Au_2^- and Au_3^- are regarded. All available theoretical literature values for the binding energies of O_2 and CO to these gold clusters are substantially larger than the RRKM data of the present contribution (with only one exception), in most cases far off of the estimated error limits of our experiment and the evaluation procedure.

Acknowledgment. Financial support by the Deutsche Forschungsgemeinschaft (SFB 450) and the Fonds der Chemischen Industrie (FCI) is gratefully acknowledged. In particular, S.M.L. thanks the FCI for a Kekulé Fellowship.

References and Notes

(1) Meyer, R.; Lemire, C.; Shaikhutdinov, S. K.; Freund, H.-J. *Gold Bull.* **2004**, *37*, 72.
(2) Haruta, M. *Nature* **2005**, *437*, 1098.
(3) Bond, G. C.; Louis, C.; Thomson, D. T. *Catalysis by Gold*; Imperial College Press: London, 2006.
(4) Min, B. K.; Friend, C. M. *Chem. Rev.* **2007**, *107*, 2709.
(5) *Nanocatalysis*; Heiz, U., Landman, U., Eds.; Springer-Verlag: Berlin, Germany, 2007.
(6) Haruta, M. *Catal. Today* **1997**, *36*, 153.
(7) Valden, M.; Lai, X.; Goodman, D. W. *Science* **1998**, *281*, 1647.
(8) Sanchez, A.; Abbet, S.; Heiz, U.; Schneider, W.-D.; Häkkinen, H.; Barnett, R. N.; Landman, U. *J. Phys. Chem. A* **1999**, *103*, 9573.
(9) *Atomic Clusters: From Gas Phase to Deposited*; Woodruff, D. P., Ed.; Elsevier: New York, 2007; Vol. 12.
(10) Pyykkö, P. *Chem. Rev.* **1988**, *88*, 563.
(11) Balasubramanian, K. *Relativistic Effects in Chemistry*; Wiley and Sons: New York, 1997.

(12) Häkkinen, H.; Moseler, M.; Landman, U. *Phys. Rev. Lett.* **2002**, *89*, 033401.
(13) Schwarz, H. *Angew. Chem., Int. Ed.* **2003**, *42*, 4442.
(14) Pyykkö, P. *Angew. Chem., Int. Ed.* **2004**, *43*, 4412.
(15) Pyykkö, P. *Inorg. Chim. Acta* **2005**, *358*, 4113.
(16) Bernhardt, T. M. *Int. J. Mass Spectrom.* **2005**, *243*, 1.
(17) Schmidbaur, H.; Cronje, S.; Djordjevic, B.; Schuster, O. *Chem. Phys.* **2005**, *311*, 151.
(18) Pyykkö, P. *Chem. Soc. Rev.* **2008**, *37*, 1967.
(19) Socaciu, L. D.; Hagen, J.; Bernhardt, T. M.; Wöste, L.; Heiz, U.; Häkkinen, H.; Landman, U. *J. Am. Chem. Soc.* **2003**, *125*, 10437.
(20) Wallace, W. T.; Whetten, R. L. *J. Am. Chem. Soc.* **2002**, *124*, 7499.
(21) Kimble, M. L.; Castleman, J., A. W.; Mitrić, R.; Bürgel, C.; Bonačić-Koutecký, V. *J. Am. Chem. Soc.* **2004**, *126*, 2526.
(22) Kimble, M. L.; Castleman, A. W., Jr.; Bürgel, C.; Bonačić-Koutecký, V. *Int. J. Mass Spectrom.* **2006**, *254*, 163.
(23) Kimble, M. L.; Moore, N. A.; Johnson, G. E.; Castleman, A. W., Jr.; Bürgel, C.; Mitrić, R.; Bonačić-Koutecký, V. *J. Chem. Phys.* **2006**, *125*, 204311.
(24) Bürgel, C.; Reilly, N. M.; Johnson, G. E.; Mitrić, R.; Kimble, M. L.; Castleman, A. W., Jr.; Bonačić-Koutecký, V. *J. Am. Chem. Soc.* **2008**, *130*, 1694.
(25) Socaciu, L. D.; Hagen, J.; Le Roux, J.; Popolan, D.; Bernhardt, T. M.; Wöste, L.; Vajda, S. *J. Chem. Phys.* **2004**, *120*, 2078.
(26) Meyer, F.; Chen, Y.-M.; Armentrout, P. B. *J. Am. Chem. Soc.* **1995**, *117*, 4071.
(27) Lee, T. H. Ph.D. Thesis, University of Nevada, 1995.
(28) Manard, M. J.; Kemper, P. R.; Bowers, M. T. *Int. J. Mass Spectrom.* **2003**, *228*, 865.
(29) Hagen, J.; Socaciu, L. D.; Heiz, U.; Bernhardt, T. M.; Wöste, L. *Eur. J. Phys. D* **2003**, *24*, 327.
(30) Lüttgens, G.; Pontius, N.; Bechthold, P. S.; Neeb, M.; Eberhardt, W. *Phys. Rev. Lett.* **2002**, *88*, 076102.
(31) Neumaier, M.; Weigend, F.; Hampe, O.; Kappes, M. M. *J. Chem. Phys.* **2005**, *122*, 104702.
(32) Neumaier, M.; Weigend, F.; Hampe, O.; Kappes, M. M. *Faraday Discuss.* **2008**, *138*, 393.
(33) Häkkinen, H.; Landman, U. *J. Am. Chem. Soc.* **2001**, *123*, 9704.
(34) Okumura, M.; Kitagawa, Y.; Haruta, M.; Yamaguchi, K. *Chem. Phys. Lett.* **2001**, *346*, 163.
(35) Lopez, N.; Norskov, J. K. *J. Am. Chem. Soc.* **2002**, *124*, 11262.
(36) Mills, G.; Gordon, M. S.; Metiu, H. *Chem. Phys. Lett.* **2002**, *359*, 493.
(37) Wells, J., D. H.; Delgass, W. N.; Kendall, T. T. *J. Chem. Phys.* **2002**, *117*, 10597.
(38) Wu, X.; Senapati, L.; Nayak, S. K.; Selloni, A.; Hajaligol, M. *J. Chem. Phys.* **2002**, *117*, 4010.
(39) Mitrić, R.; Bürgel, C.; Burda, J.; Bonačić-Koutecký, V.; Fantucci, P. *Eur. J. Phys. D* **2003**, *24*, 41.
(40) Yoon, B.; Häkkinen, H.; Landman, U. *J. Phys. Chem. A* **2003**, *107*, 4066.
(41) Varganov, S. A.; Olson, R. M.; Gordon, M. S.; Metiu, H. *J. Chem. Phys.* **2003**, *119*, 2531.
(42) Varganov, S. A.; Olson, R. M.; Gordon, M. S.; Mills, G.; Metiu, H. *Chem. Phys. Lett.* **2003**, *368*, 778.
(43) Ding, X.; Dai, B.; Yang, J.; Hou, J. G.; Zhu, Q. *J. Chem. Phys.* **2004**, *121*, 621.
(44) Ding, X.; Li, Z.; Yang, J.; Hou, J. G.; Zhu, Q. *J. Chem. Phys.* **2004**, *120*, 9594.
(45) Phala, N. S.; Klatt, G.; van Steen, E. *Chem. Phys. Lett.* **2004**, *395*, 33.
(46) Molina, L. M.; Hammer, B. *J. Chem. Phys.* **2005**, *123*, 161104.
(47) Joshi, A. M.; Delgass, W. N.; Thomson, K. T. *J. Phys. Chem. B* **2006**, *110*, 23373.
(48) Joshi, A. M.; Tucker, M. H.; Delgass, W. N.; Thomson, K. T. *J. Chem. Phys.* **2006**, *125*, 194707.
(49) Luo, C.; Fa, W.; Dong, J. *J. Chem. Phys.* **2006**, *125*, 084707.
(50) Prestianni, A.; Martorana, A.; Labat, F.; Ciofini, I.; Adamo, C. *J. Phys. Chem. B* **2006**, *110*, 12240.
(51) Wang, Y.; Gong, X. G. *J. Chem. Phys.* **2006**, *125*, 124703.
(52) Chen, Y.; Crawford, P.; Hu, P. *Catal. Lett.* **2007**, *119*, 21.
(53) Mitrić, R.; Bürgel, C.; Bonačić-Koutecký, V. *Proc. Natl. Acad. Sci. U.S.A.* **2007**, *104*, 10314.
(54) Okumura, M.; Haruta, M.; Kitagawa, Y.; Yamaguchi, K. *Gold Bull.* **2007**, *40*, 40.
(55) Schwerdtfeger, P.; Lein, M.; Krawczyk, R. P.; Jacob, C. R. *J. Chem. Phys.* **2008**, *128*, 124302.
(56) Torres, M. B.; Fernández, E. M.; Balbás, L. C. *J. Phys. Chem. A* **2008**, *112*, 6678.
(57) Hagen, J.; Socaciu, L. D.; Elijazyfer, M.; Heiz, U.; Bernhardt, T. M.; Wöste, L. *Phys. Chem. Chem. Phys.* **2002**, *4*, 1707.
(58) Hagen, J.; Socaciu, L. D.; Le Roux, J.; Popolan, D.; Bernhardt, T. M.; Wöste, L.; Mitrić, R.; Noack, H.; Bonačić-Koutecký, V. *J. Am. Chem. Soc.* **2004**, *126*, 3442.
(59) Socaciu, L. D. Ph.D. Thesis, Freie Universität, Berlin, Germany, 2004.
(60) Hagen, J. Ph.D. Thesis, Freie Universität, Berlin, Germany, 2004.
(61) Bernhardt, T. M.; Socaciu-Siebert, L. D.; Hagen, J.; Wöste, L. *Appl. Catal., A* **2005**, *291*, 170.
(62) Socaciu, L. D.; Hagen, J.; Heiz, U.; Bernhardt, T. M.; Leisner, T.; Wöste, L. *Chem. Phys. Lett.* **2001**, *340*, 282.
(63) Keller, R.; Nöhmeier, F.; Spädtke, P.; Schönenberg, M. H. *Vacuum* **1984**, *34*, 31.
(64) Reynolds, O. *Philos. Trans. R. Soc. London* **1879**, *10*, 727.
(65) Maxwell, J. C. *Philos. Trans. R. Soc. London* **1879**, *170*, 231.
(66) Loriot, G.; Moran, T. *Rev. Sci. Instrum.* **1975**, *46*, 140.
(67) Bell, R. C.; Zemski, K. A.; Justes, D. R.; Castleman, A. W., Jr. *J. Chem. Phys.* **2001**, *114*, 798.
(68) Miller, T. A. *J. Phys. Chem.* **1963**, *67*, 1359.
(69) Wu, Y. *J. Chem. Phys.* **1968**, *48*, 889.
(70) Carr, P. H. *Vacuum* **1964**, *14*, 37.
(71) Hobson, J. P. *J. Vac. Sci. Technol.* **1969**, *6*, 257.
(72) Hobson, J. P. *J. Vac. Sci. Technol.* **1970**, *7*, 351.
(73) Schumacher, E. DETMECH - Chemical Reaction Kinetics Software, University of Bern, 2003 (http://www.chemsoft.ch).
(74) Sun, Q.; Jena, P.; Kim, Y. D.; Fischer, M.; Ganteför, G. *J. Chem. Phys.* **2004**, *120*, 6510.
(75) Kim, Y. D.; Ganteför, G. *Chem. Phys. Lett.* **2004**, *383*, 80.
(76) Steinfeld, J. I.; Francisco, J. S.; Hase, W. L. *Chemical Kinetics and Dynamics*, 2nd ed.; Prentice Hall: Upper Saddle River, NJ, 1999.
(77) Langevin, P. M. *Ann. Chem. Phys.* **1905**, *5*, 245.
(78) Castleman, A. W., Jr.; Weil, K. G.; Sigsworth, S. W.; Leuchtner, R. E.; Keesee, R. G. *J. Chem. Phys.* **1987**, *86*, 3829.
(79) Su, T.; Chesnavich, W. J. *J. Chem. Phys.* **1982**, *76*, 5183.
(80) Gioumousis, G.; Stevenson, D. P. *J. Chem. Phys.* **1958**, *29*, 294.
(81) Marcus, R. A. *J. Chem. Phys.* **1952**, *20*, 359.
(82) Holbrook, K. A.; Pilling, M. J.; Robertson, S. H. *Unimolecular Reactions*, 2nd ed.; John Wiley & Sons Ltd.: Chichester, U.K., 1996.
(83) Cox, D. M.; Reichmann, K. C.; Trevor, D. J.; Kaldor, A. *J. Chem. Phys.* **1988**, *88*, 111.
(84) Drahos, L.; Vekey, K. *J. Mass Spectrom.* **2001**, *36*, 237.
(85) Marcus, R. *J. Chem. Phys.* **1965**, *43*, 2658.
(86) Bonačić-Koutecký, V. Private communication.
(87) Spasov, V. A.; Lee, T. H.; Maberry, J. P.; Ervin, K. M. *J. Chem. Phys.* **1999**, *110*, 5208.
(88) Shvartsburg, A. A.; Ervin, K. M.; Frederick, J. H. *J. Chem. Phys.* **1996**, *104*, 8458.
(89) Bonačić-Koutecký, V.; Burda, J.; Mitrić, R.; Ge, M.; Zampella, G.; Fantucci, P. *J. Chem. Phys.* **2002**, *117*, 3120.
(90) Leuchtner, R. E.; Harms, A. C.; Castleman, A. W., Jr. *J. Chem. Phys.* **1990**, *92*, 6527.
(91) Campbell, C. T. *Surf. Sci.* **1985**, *157*, 43.
(92) Upton, T. H.; Stevens, P.; Madix, R. J. *J. Chem. Phys.* **1988**, *88*, 3988.
(93) Backx, C.; De Groot, C. P. M.; Biloen, P. *Surf. Sci.* **1981**, *104*, 300.
(94) Garfunkel, E. L.; Ding, X.; Dong, G.; Yang, S.; Hou, X.; Wang, X. *Surf. Sci.* **1985**, *164*, 511.
(95) Shi, Y.; Spasov, V. A.; Ervin, K. M. *J. Chem. Phys.* **1999**, *111*, 938.
(96) Baer, T.; Mayer, P. M. *J. Am. Soc. Mass Spectrom.* **1997**, *8*, 103.
(97) Jarrold, M. F.; Bower, J. E. *J. Chem. Phys.* **1987**, *87*, 5728.
(98) Lee, T. H.; Ervin, K. M. *J. Phys. Chem.* **1994**, *98*, 10023.
(99) Cox, D. M.; Brickman, R.; Creegan, K.; Kaldor, A. *Z. Phys. D* **1991**, *19*, 353.
(100) Cox, D. M.; Brickman, R. O.; Creegan, K.; Kaldor, A. *Mater. Res. Soc. Symp. Proc.* **1991**, *206*, 43.
(101) Salisbury, B. E.; Wallace, W. T.; Whetten, R. L. *Chem. Phys.* **2000**, *262*, 131.
(102) Wallace, W. T.; Wyrwas, R. B.; Whetten, R. L.; Mitrić, R.; Bonačić-Koutecký, V. *J. Am. Chem. Soc.* **2003**, *125*, 8408.
(103) Wallace, W.; Leavitt, A. J.; Whetten, R. L. *Chem. Phys. Lett.* **2003**, *368*, 774.
(104) Ho, J.; Ervin, K. M.; Lineberger, W. C. *J. Chem. Phys.* **1990**, *93*, 6987.
(105) Handschuh, H.; Cha, C.-Y.; Bechthold, P. S.; Ganteför, G.; Eberhardt, W. *J. Chem. Phys.* **1995**, *102*, 6406.
(106) Negishi, Y.; Nakamura, Y.; Nakajima, A.; Kaya, K. *J. Chem. Phys.* **2001**, *115*, 3657.
(107) Handschuh, H.; Ganteför, G.; Bechthold, P. S.; Eberhardt, W. *J. Chem. Phys.* **1994**, *100*, 7093.
(108) Häkkinen, H.; Yoon, B.; Landman, U.; Li, X. L.; Zahi, H.-J.; Wang, L.-S. *J. Phys. Chem. A* **2003**, *107*, 6168.

(109) Taylor, K. J.; Pettiette-Hall, C. L.; Cheshnovsky, O.; Smalley, R. E. *J. Chem. Phys.* **1992**, *96*, 3319.
(110) Yuan, D. W.; Zeng, Z. *J. Chem. Phys.* **2004**, *120*, 6574.
(111) Elschenbroich, C.; Salzer, A. *Organometallics*; VCH: Weinheim, Germany, 1989.
(112) Lian, L.; Hackett, P. A.; Rayner, D. M. *J. Chem. Phys.* **1993**, *99*, 2583.
(113) Lee, H. M.; Ge, M.; Sahu, B. R.; Tarakeshwar, P.; Kim, K. S. *J. Phys. Chem. B* **2003**, *107*, 9994.
(114) Wallace, W. T.; Whetten, R. L. *J. Phys. Chem. B* **2000**, *104*, 10964.
(115) Wallace, W. T.; Whetten, R. L. *Eur. J. Phys. D* **2001**, *16*, 123.

JP810055Q